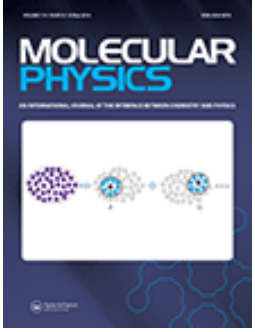

Taylor & Francis
Taylor & Francis Group

Molecular Physics

An International Journal at the Interface Between Chemistry and Physics

ISSN: 0026-8976 (Print) 1362-3028 (Online) Journal homepage: https://www.tandfonline.com/loi/tmph20

# Constant chemical potential, pressure and temperature profiles in liquid–vapour equilibrium obtained by spinodal decomposition

Enrique Díaz-Herrera, Anthony Bryan Gutiérrez & Gustavo A. Chapela

**To cite this article:** Enrique Díaz-Herrera, Anthony Bryan Gutiérrez & Gustavo A. Chapela (2020): Constant chemical potential, pressure and temperature profiles in liquid–vapour equilibrium obtained by spinodal decomposition, Molecular Physics, DOI: 10.1080/00268976.2020.1711975

**To link to this article:** https://doi.org/10.1080/00268976.2020.1711975

Published online: 15 Jan 2020.

MOLECULAR PHYSICS
https://doi.org/10.1080/00268976.2020.1711975

Taylor & Francis
Taylor & Francis Group

RESEARCH ARTICLE



# Constant chemical potential, pressure and temperature profiles in liquid–vapour equilibrium obtained by spinodal decomposition

Enrique Díaz-Herrera[a], Anthony Bryan Gutiérrez[b] and Gustavo A. Chapela[a]

[a]Departamento de Física, Universidad Autónoma Metropolitana-Iztapalapa, México D.F., México; [b]Doctorado en Química, Universidad Autónoma Metropolitana-Iztapalapa, México D.F., México

**ABSTRACT**

Constant chemical potential, pressure and temperature profiles across a slab of liquid in equilibrium with its vapour confirm that, the spinodal decomposition procedure carried on the NVT ensemble simulated via molecular dynamics produce an equilibrium system. An initial homogeneous crystalline configuration of fluid is kept in a cell with a parallelepiped shape at a density near the critical density and a temperature between the triple and critical temperatures, form a slab of liquid in equilibrium with its vapour by the spinodal decomposition phenomenon if the simulation is performed in the NVT ensemble. An elongated box favours the formation of two planar parallel surfaces along the largest side of the box. We show in this paper that the 'three conditions' for thermodynamic equilibrium: constant temperature, constant pressure and constant chemical potential are met for such a system.

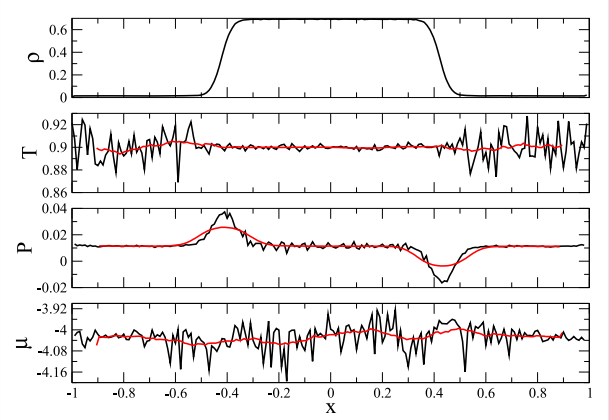


**ARTICLE HISTORY**
Received 24 September 2019
Accepted 16 December 2019

**KEYWORDS**
Liquid–vapour equilibrium; chemical potential profile; spinodal decomposition; molecular dynamics simulation

## 1. Introduction

There have been several approaches to analyse the liquid–vapour equilibrium (LVE) of a fluid interacting with an attractive potential such as the Lennard–Jones (LJ) or the Square Well (SW) potentials via molecular simulation. Hansen and Verlet [1], in 1969, were the first to calculate the LVE of a LJ fluid using a constrained Monte Carlo (MC) method. In the next decade, the first attempt to calculate the interphase, the orthobaric curve and the surface tension via molecular simulation was made by John Rowlinson's group in 1975–1977 [2,3]. They used MC and molecular dynamics (MD) on an elongated box closed in the two most separated sides simulated in the NVT ensemble. This approach was further refined in 1987, using the spinodal decomposition (SD) phenomenon by Chapela et al. [4], which uses also an elongated box simulated in the NVT ensemble, but in this case, it is open in all dimensions. Rao et al. [5,6] were the first to calculate the pressure profiles (the tangential and the normal) for a planar interphase of an LJ fluid with a cutoff of 2.5 diameters. They concluded that the position of the surface tension was located at a distance of 0.04 diameters from the Gibbs dividing surface. Adams, in 1979, [7] obtained results for the LVE with a grand canon-

**CONTACT** Gustavo A. Chapela gchapela@xanum.uam.mx Departamento de Física, Universidad Autónoma Metropolitana-Iztapalapa, Av. San Rafael Atlixco 186, Col. Vicentina, México D.F. 09340, México

ical MC technique (GCMC), and Nicolas et al. [8] managed to obtained the same results via an equation of state for the whole region. In 1987, a breakthrough occurred when Panagiotopoulus [9] proposed his seminal method of the Gibbs ensemble MC technique (GEMC). It has become one of the most popular and useful methods to obtain LVE properties. Lofti et al. [10] in 1990 put forward a method which combines an NpT MC simulation with a Widom [11] particle insertion procedure to get the LVE quantities. Even though it is not directly related to the topic of LVE calculation, the contribution of the method of finite size scaling in 1992 by Wilding et al. [12], which is used to accurately calculate the critical point of a fluid, deserves a mention. The Gibbs-Duhem integration, introduced by Kofke [13] in 1993 is also an important contribution which combines a molecular simulation, normally MC in the NVT ensemble, and a thermodynamic integration using the Gibbs-Duhem equation. The surface tension of a LVE was calculated with an area sampling MC or MD, introduced by Gloor et al. [14] in 2005. This Introduction gives a tight account of the development of the procedures employed in the calculation to obtain the LVE of a pure fluid. For a comprehensive review on the calculation of surface tension via molecular simulation, see Ghoufi et al. [15].

The method that will be used in this work if the SD procedure with an elongated box [4] with periodic boundary conditions in all directions simulated in the NVT ensemble. The initial configuration is usually an homogeneous crystal at a density near the critical and a temperature between the critical and the triple point temperatures. The SD produces a slab of liquid which is presumed to be in equilibrium with its vapour. This choice of initial global density promotes, according to Maxwell's lever rule, the formation of equivalent quantities of liquid and vapour, providing two very well defined liquid interphases due to the imposed periodic conditions. Even though the SD method has been reported having significant drawbacks [16] it has been used in many calculations on the surface properties of LVE [17–19] to cite only a few. As an example of this comments, here is a quote taken from a paper by Vega et al. [16] where they report the VLE of the SW fluid in three dimensions using a GEMC procedure. They refer to papers by Chapela et al. [4] and Benavides et al. [17]:

> However, these types of direct simulation studies of phase equilibria possess significant drawbacks because the method is restricted to a film of liquid confined between parallel plates. Unless the size of the system is very large the confinement causes the coexistence properties of the fluid to be different from the bulk coexistence properties of interest. In fact, the method breaks down altogether for temperatures close to the critical point.

The initial procedure used a closed box but the version based on the SD phenomena [4] used an open elongated box. Also one could add that all methods break down near the critical point exception made of the finite size scaling of Wilding et al. [12], which was properly designed to be used in the vicinity of the critical point. This is a property of the critical point rather than a drawback of any method. Another characteristic of the SD method is that an explicit density profile is provided by the simulation. In fact two liquid–vapour interphases are formed, in contrast with most other methods that do not provide one, for example, see Sing et al. [20].

The comment in print [16] and others made to us verbally by colleges, in terms that the system is not proven to be in equilibrium, prompted us to try and test the equilibrium property of the SD method. In order to do this, we calculated the temperature, pressure and chemical potential profiles of the LJ and SW fluids, which by the way, is the only method that gives the liquid and the coexisting vapour, forming a planar interphase. Previously, Trokhymchuk and Alejandre [18] reported the pressure profiles for the LJ fluid with several cut off distances of the potential calculated with Monte Carlo and molecular dynamics methods, establishing the unequivocal condition of mechanical equilibrium of the systems. Imre et al. [19] used the SD method checked thermal equilibrium with the temperature profile but they do not show it. No chemical potential profiles have been found.

The main aim of this work is to show that the SD technique produces an equilibrated liquid–vapour system. To do it we propose to calculate the temperature, pressure and chemical potential profiles across the interphase and show that they are horizontal lines, except across the two interphases in the system.

The work is organised as follows. After Section 1, Section 2 describes the LJ and the SW potentials. Section 3 describes the Methods used: the Widom test particle, the SD procedure and the NVT MD simulation follow. Section 4 explains how the temperature, pressure and chemical potential profiles are calculated is given next and Sections 5 and 6 and 7 describe Results and Conclusions, respectively, which close the work. The Results section makes special emphasis in the comparison of the results of LJ and SW systems.

## 2. Interaction models

We used the LJ Equation (1) and the SW Equation (3) potentials to test the hypothesis of the system being in equilibrium. These two potentials are the simplest and the most used attractive potentials. Figure 1 shows a pictorial representation of both.

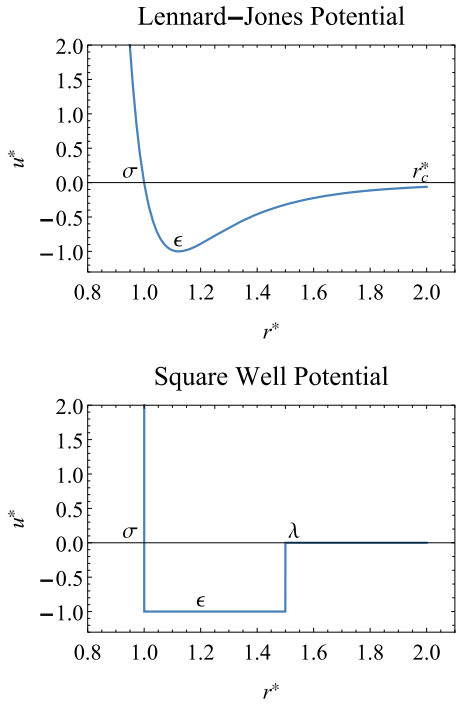


**Figure 1.** LJ and SW interaction potentials.

The truncated and shifted LJ potential $u_{\mathrm{LJ}}(r)$ is:

$$u_{\mathrm{LJ}}(r) = 4\epsilon\left[\left(\frac{\sigma}{r}\right)^{12} - \left(\frac{\sigma}{r}\right)^{6}\right] \tag{1}$$

with:

$$u_{\mathrm{LJ_{TS}}}(r) = \begin{cases} u_{\mathrm{LJ}}(r) - u_{\mathrm{LJ}}(r_c) & \text{if } r \le r_c \\ 0 & \text{if } r > r_c \end{cases} \tag{2}$$

and the SW potential $u_{\mathrm{SW}}(r)$ is given by:

$$u_{\mathrm{SW}}(r) = \begin{cases} \infty & \text{if } r \le \sigma \\ -\epsilon & \text{if } \sigma < r \le \lambda \\ 0 & \text{if } r > \lambda \end{cases} \tag{3}$$

For the rest of the work when we refer to the LJ potential, it means the truncated and shifted LJ potential. Where $r$ is the dimensionless distance and $\sigma$ and $\epsilon$ are the distance and energy constants of the potentials. Standard dimensionless units in terms of the parameters $\sigma$ and $\epsilon$ for distance and energy are used throughout the work.

## 3. Methods

There are at least eight methods to calculate LVE properties. In this work, we focus our attention in the SD procedure [4] performed in an open elongated simulation box with periodic boundary conditions in all directions to obtain a liquid slab in equilibrium with its vapour, at temperatures between the critical and the triple point. As the main aim of this work is to show that this method brings a system to thermodynamic equilibrium if sufficient time is allowed in the simulation, the particle insertion method devised by Widom [11] is used to calculate the chemical potential profile which is described in detail in the next section. The NVT ensemble MD simulation is also described for both versions, the continuous one by Verlet [21] and the molecular dynamics of discontinuous potentials (MDDP) version put forward by Alder et al. [22], modified by Rapaport [23] and extended to molecules and mixtures by Chapela et al. [24]

### 3.1. Widom particle insertion method

Ben Widom [11] devised his particle insertion method to calculate the chemical potential in 1963. It consists in inserting a particle in the fluid and obtaining its potential energy, the sum of all the interaction energies of the inserted particles with the rest of the fluid is used to evaluate the work needed to insert such a particle. The chemical potential $\mu$ at a temperature $T$ and density $\rho = N/V$, is then the work needed to insert such particle given as:

$$\mu/k_bT = -\ln\left\langle V\ \exp(-\beta\phi)\right\rangle/N \tag{4}$$

where $\phi$ is the total potential energy of the inserted particle and the brackets represent the ensemble average in the isobaric-isothermal ensemble. The number of particles and the volume are $N$ and $V$, respectively. The symbol $\beta = 1/k_bT$ with $k_b$ being the Boltzmann's constant. This method was applied to the resulting configurations after a lengthy enough period of equilibration, (typically of 100 000 time steps for the LJ fluid and 10 million collisions for the SW fluid) 1000 insertions in each slab were tried for each of a 5000 configurations taken at least 5000 time steps apart for LJ and, 4000 insertions in each slab on 1225 configurations of 4 million collisions each for SW.

### 3.2. Spinodal decomposition method

The SP method [4] is normally conducted in an NVT ensemble starting with some crystalline initial configuration at a density close to the critical density of the fluid to be studied and a temperature between the critical and triple point temperatures. The SD is performed in an elongated simulation box with periodical boundaries in all directions. The initial positions of the atoms are given as a crystalline array. A slab of liquid is formed in the cell with both planar interphases being perpendicular to the longest side of the box. The initial density close to the critical is fixed to insure a proper formation of a liquid slab at the desired temperature. It is known that

away from the critical density spheres or cylinders can be formed [25,26]. The SD phenomenon occurs in a matter of 1 to 2 pico seconds [4,27]. This is equivalent to 10,000 time steps for LJ and 100,000 collisions for SW. After this initial SD period, an equilibration period was allowed as mentioned in the previous Section.

### 3.3. Molecular dynamics in the NVT ensemble

This is a usual procedure whose description can be obtained readily elsewhere for the velocity Verlet algorithm [21] and for the MDDP [22–24]. An FCC array at the proper density and temperature is used as initial condition. After an appropriate period of SD simulation and an equilibration period of length mentioned above are allowed, a total size of the simulations was of around 0.5 million time steps for LJ and at least 10 blocks of 4 million collisions for the SW runs.

## 4. Calculated properties

Temperature, pressure and chemical potential profiles are the main calculated properties in this work. In order to obtain a profile, the box in the largest direction is divided into small slices of $0.1\sigma$ ($0.05\sigma$ for the case of the LJ potential) and the corresponding property is calculated for that slice.

Temperature $T$ is obtained via the definition

$$T = \frac{2\langle E_k \rangle}{N n_d} \tag{5}$$

where $E_k$ is the kinetic energy, $N$ is the number of particles and $n_d$ is the number of degrees of freedom, the dimensionality of the system.

Pressure profile is obtained with the pressure tensor components normal to the surface $P_N(x)$ and tangential to the surface $P_T(x)$, which are calculated using the Irving and Kirkwood [6,28–31] definition for the LJ potential as:

$$P_N(x) = \langle \rho(x) \rangle k_b T - \frac{1}{A} \left\langle \sum_i \sum_{j>i} \frac{|x_{ij}|}{r_{ij}} \frac{dU_{LJ}(r_{ij})}{dr_{ij}} \times \theta\left(\frac{x - x_i}{x_{ij}}\right) \theta\left(\frac{x_j - x}{x_{ij}}\right) \right\rangle \tag{6}$$

$$P_T(x) = \langle \rho(x) \rangle k_b T - \frac{1}{A} \left\langle \sum_i \sum_{j>i} \frac{(y_{ij}^2 + z_{ij}^2)}{2 r_{ij}} \frac{dU_{LJ}(r_{ij})}{dr_{ij}} \frac{1}{|x_{ij}|} \times \theta\left(\frac{x - x_i}{x_{ij}}\right) \theta\left(\frac{x_j - x}{x_{ij}}\right) \right\rangle \tag{7}$$

where $\langle \rho(x) \rangle$ is the ensemble average of the density profile in the largest direction of the box, $k_b$ and $T$ are the Boltzmann constant and the temperature, $A$ the area of the box in the y-z plane, and $dU_{\mathrm{LJ}}(r_{ij})/dr_{ij}$ the LJ force.

The Clausius' virial theorem [32] is used to calculate the pressure tensor components normal to the surface $P_N(x) = P_x(x)$ and tangential to the surface $P_T(x) = (P_y(x) + P_z(x))/2$ for the SW potential as the ensemble average of the momentum transfer at every collision as:

$$P_\alpha(x) = \langle \rho(x) \rangle k_b T - \frac{1}{At} \left\langle \sum_{col's} m_i \Delta v_{\alpha_{ij}} \alpha_{ij} / |x_{ij}| \times \theta\left(\frac{x - x_i}{x_{ij}}\right) \theta\left(\frac{x_j - x}{x_{ij}}\right) \right\rangle \tag{8}$$

where $P_\alpha(x)$ and $\alpha ij$ are the instantaneous component of the pressure tensor and the distance between particles $i$ and $j$ in the $\alpha$ direction, respectively, $A$ is the transversal area of the simulation box, $t$ is the simulation elapsed time between collisions, $\Delta v_{\alpha_{ij}}$ is the $\alpha$ component of the velocity vector difference of the colliding pair of particles $i$ and $j$ before and after the collision, and $x_{ij}$ is the $x$ component of the vector joining the centres of the two atoms. $x_j$ and $x_j$ are the $x$ coordinates of particles $i$ and $j$. This equation applies to components $P_y(x)$ and $P_z(x)$ of the pressure tensor.

In the case of a planar interface the pressure tensor is diagonal, but not homogeneous. It can be decompose in a normal component (normal to the interface) which corresponds to the pressure of the system $P = P_N + \rho T$, and a parallel or tangential component $P_T$, which can be written as: $P_T = (1/2)(\tau_{yy} + \tau_{zz}) + \rho T$ and $P = \tau_{xx} + \rho T$, where $\tau_{ab}$ corresponds to element $ab$ of the pressure tensor. For the case of an homogeneous fluid, pressure reduces to $P = \frac{1}{3}(\tau_{xx} + \tau_{yy} + \tau_{zz}) + \rho T$, the mean of the diagonal components of the pressure tensor, with $\tau_{xx} = \tau_{yy} = \tau_{zz}$ plus the ideal gas pressure.

Chemical potential profile $\mu(x)$ is obtained with the Widom [11] insertion particle (IP) method. The potential energy of each inserted particle is used to calculate the work that is needed to insert such particle in the midst of the fluid. The relation used is:

$$\mu(x) = \mu_{ex}(x) + T \ln(\rho(x)) \tag{9}$$

where $\mu_{ex}(x)$ is given by:

$$\mu_{ex}(x) = -T \ln\left(\langle W_{test}(x) \rangle\right) \tag{10}$$

with

$$W_{test}(x)) = \exp(-T \Delta U(x)) \tag{11}$$

and,

$$\Delta U(x) = U_{N+1}(x) + U_N(x). \tag{12}$$

where $\beta = 1/T$, $\phi(x)$ is the potential energy profile of the inserted particles, and $\rho(x)$ is the density profile, obtained as:

$$\rho(x) = \left\langle \frac{N(x)}{A\Delta x} \right\rangle \tag{13}$$

where $N(x)$ is the number of particles in a slab with area $A = L_y L_z$ and thickness $\Delta x$.

## 5. Results for the LJ fluid

As mentioned above, this work is dedicated to show that a fluid with attractive interactions processed with MD in the NVT ensemble reaches effective thermodynamic equilibrium when simulated in an open elongated cell (periodic boundary conditions in all directions) within the coexistence region. The inhomogeneous fluid is created, by a SD process, with liquid and vapour phases divided by an interface with finite surface tension. The parallelepiped shape of the cell is used to favour the formation of a planar interface normal to its largest direction. Mechanical equilibrium is achieved, as has been shown by Trokhymchuk and Alejandre [18] in the planarity of their reported pressure profiles across the interface. What has been missing since then is to show that chemical and thermal equilibrium are also achieved, this will be done by calculating the chemical potential and temperature profiles of the same system mentioned above. Constant temperature, pressure and chemical equilibrium are the thermodynamic conditions to achieve an equilibrated state. Henceforth, planar profiles of these three properties assure the equilibrium state of the coexisting liquid–vapour system has been reached. We used a LJ fluid simulated in an elongated box of dimensions $L_x$, $L_y$, $L_z$ with $L_x = 2L_y$, to show that the final liquid–vapour system is equilibrated. A system containing 5000 particles was simulated. The cutoff diameter for the LJ was $R_c = 3\sigma$ at a selected temperature of $T = 0.9$ which lays at half point between the triple point $T_t = 0.6$ and the critical point $T_c = 1.15$, [16] was chosen. The initial density is the critical density $\rho = 0.3$. A shifted LJ potential is used in all simulations. It is worth noticing that a molecular truncated force model cutoff, corresponds analytically to a shifted potential energy with a similar cutoff.

### 5.1. Results for $T = 0.9$ and $\rho = 0.3$

Figure 2 shows from top to bottom, density, temperature, pressure and chemical potential profiles.

A temperature of $T = 0.9$ at an overall density of $\rho = 0.3$ were chosen to simulate the LJ system with 5000 particles. The noisier lines represent the actual results obtained from 10,000 con gurations of the simulation over 0.5 million time steps with partial results taken every 50 time steps, which explains the noisy results. Less noisy lines are mean values taken for every 50 slabs. The noise

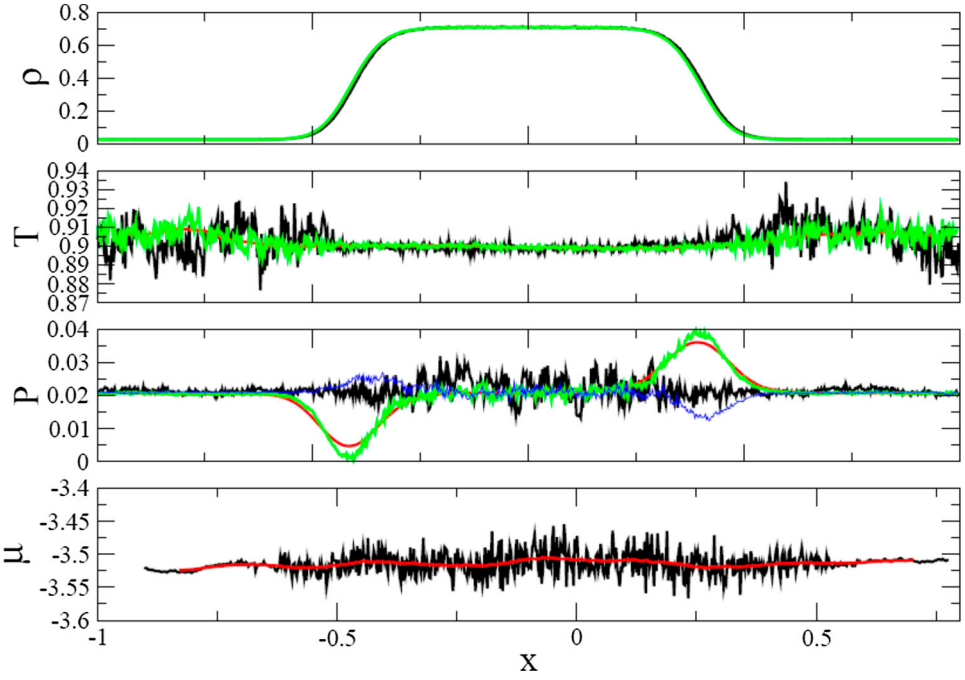


**Figure 2.** LJ profiles. From the top down, density, temperature, pressure and chemical potential profiles at $T = 0.9$ and $\rho = 0.3$ are shown.

has disappeared and the profi les are quite smooth. Lines with minima and maxima represent two independent runs with results averaged over 100,000 con figurations of simulations with 5 million time steps with partial results taken every 50 time steps, which gives much less noisier results. These lines are an indication of long term noise.

The density profile is quite smooth for both runs, giving liquid and vapour densities of $\rho_l = 0.707 \pm 0.001$ and $\rho_v = 0.0277 \pm 0.0005$, respectively. Temperature profile is quite smooth in the liquid portion and noisier in the vapour side for the short run and both are much more smoother for the longer run. For this run the values of the mean temperature of the liquid an the vapour corresponding to $T_l = 0.8994 \pm 0.0006$ and $T_v = 0.906 \pm 0.004$, respectively. Pressure profile are noisier for the short run (black line) and much less noisier for both the longer runs (green and blue lines). The maxima and minima of the pressure are of opposite signs reinforcing its noisy origin. Mean values for the pressure in the liquid and vapour as $P_l = 0.021 \pm 0.001$ and $P_v = 0.0206 \pm 0.0002$, respectively. The chemical potential profile is quite noisy and no attempt was done to perform a longer run since we are convinced that this noise is just that, noise. Chemical potential mean values for both phases are $\mu_l = -3.509 \pm 0.015$ and $\mu_v = -3.516 \pm 0.006$. Pressure profile shows a minimum through the interface in the left an a maximum when crossing the interface to the right. The mean values of temperature, pressure and chemical potential profiles in both phases are within their statistical error. All profiles are planar enough to support our point of equilibrium.

## 6. Results for the SW fluid

An SW potential with parameters of $\sigma = \epsilon = 1$ and $\lambda = 1.5\sigma$ was simulated. A similar initial configuration of the LJ case containing 5000 particles as an homogeneous fcc crystal at a density $\rho = 0.3$ was used. This initial density is close to the critical density of the SW fluid $\rho_c = 0.299 \pm 0.023$. A temperature of $T = 0.9$ which lays between the triple point $T_t = 0.6$ and the critical point temperature $T_c = 1.219 \pm 0.016$, was selected to simulate the system. The critical pressure is $P_c = 0.108 \pm 0.008$. (Critical constants were taken from Ref. [16]). An elongated box of dimensions $L_x, L_y, L_z$ with $L_x = 2L_y$ was chosen also. The SD procedure was used to produce a slab with two parallel planar surfaces of liquid in equilibrium with its vapour. We and everybody else that have used this procedure suppose that the outcome is an equilibrated configuration. Our aim, as stated before, is to show that this is the case, calculating the temperature, pressure and chemical potential profiles along and across the perpendicular direction of the liquid slab.

### 6.1. Results for $T = 0.9$ and $\rho = 0.3$

Figure 3 shows from top to bottom, density, temperature, pressure and chemical potential profiles at a temperature os $T = 0.9$ and a global density of $\rho = 0.3$ obtained using the SD procedure. Noisier lines represent the actual results obtained from the simulation after 2,500 blocks of 4 million collisions with partial results calculated every block (exception made of the pressure

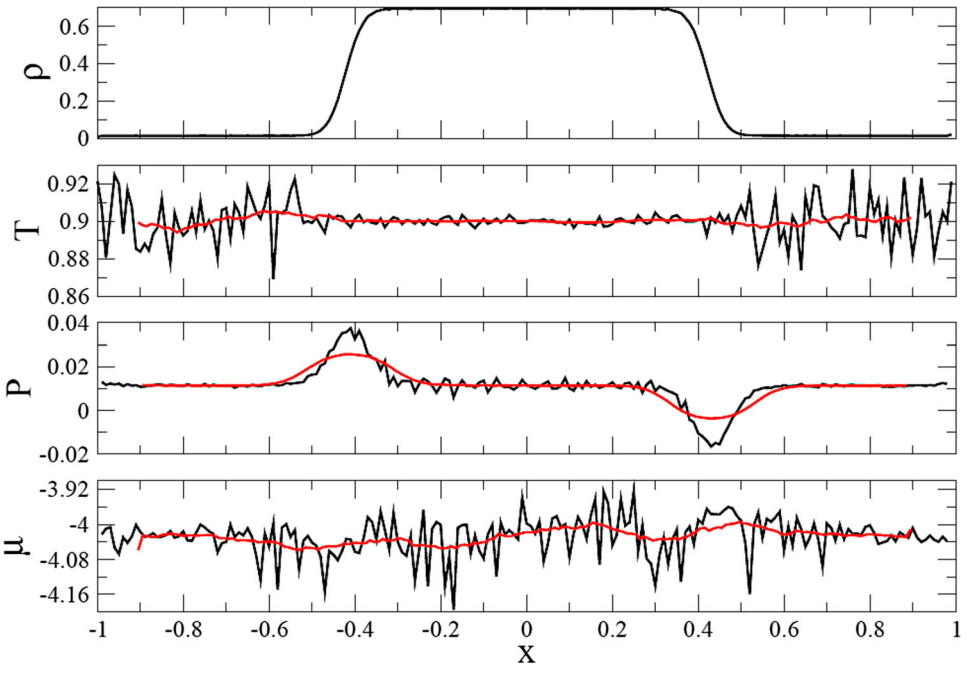


**Figure 3.** SW profiles. From the top down, density, pressure and chemical potential profiles at $T = 0.9$ and $\rho = 0.3$ are shown.

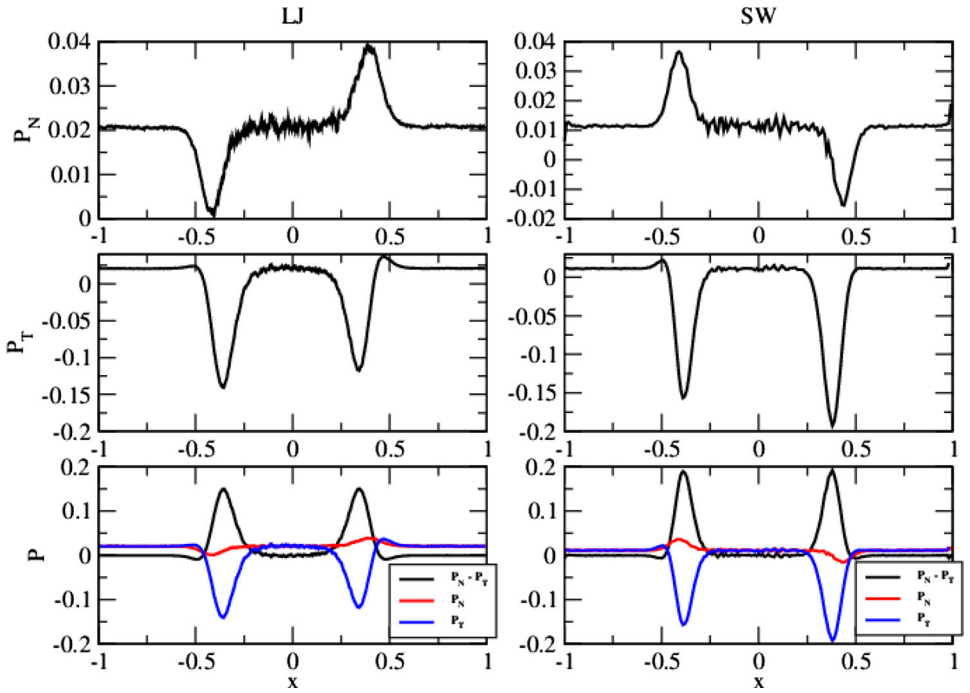


**Figure 4.** $P_N$, $P_T$ and $P_N - P_T$ profiles. For LJ (left) and SW (right) at $T = 0.9$ and $\rho = 0.3$, performed with 5000 particles. Averages taken for 100 000 configurations for LJ and for 2500 blocks of 4 million collisions for SW. The three profiles drawn together to emphasise the difference in scale for the three profiles. Maximum and minimum for $P_N$ are small compared with their $P_T$ counterpart.

whose contributions were accumulated at every collision). Smoother lines are mean values taken for every 25 slabs. The noise has disappeared.

As in the case of LJ, the density profile is quite smooth. The black line represents the actual results obtained from the simulation after 2500 blocks of 4 million of collisions with partial results taken every block, except for the case of the pressure whose contributions were accumulated at every collision. The liquid and vapour densities obtained from the profile are: $\rho_l = 0.6923 \pm 0.0006$ and $\rho_v = 0.0146 \pm 0.0006$, respectively. The temperature profile is also quite smooth in the liquid portion and noisier in the vapour side due to the small quantity of atoms in the vapour phase with values of the mean temperature of the liquid an the vapour corresponding to $T_l = 0.900 \pm 0.001$ and $T_v = 0.90 \pm 0.01$, respectively. Pressure and chemical potential profiles are noisier because these properties have larger fluctuations with mean values for the pressure in the liquid and vapour as $P_l = 0.011 \pm 0.001$ and $P_v = 0.0114 \pm 0.0003$, respectively; and mean values for the chemical potential in both phases as $\mu_l = -4.02 \pm 0.04$ and $\mu_v = -4.03 \pm 0.02$. Again, as in the case of the LJ fluid, both profiles are planar enough to make our point of equilibrium.

The pressure profile is smoother than its LJ counterpart mainly due to the wider slabs used and that every collision is taken into account in calculating the mean values. It presents a maximum and a minimum, just like its LJ counterpart, but in this case it seems to have converged. We have run it for at another run as long as the first and the maximum and minimum remain the same. The values for the liquid $P_l = 0.011 \pm 0.001$ and for the vapour $P_v = 0.0114 \pm 0.0003$. The chemical potential profile is noisier because it has larger fluctuations and the configurations used to calculate the mean were only 1225. The chemical potentials are for the liquid phase $\mu_l = -4.02 \pm 0.04$ and for the vapour phase $\mu_v = -4.03 \pm 0.02$. This profile is planar enough to support our point of equilibrium.

Figure 4 shows the components of the pressure tensor of the LJ fluid (left) and of the SW fluid (right). From top to bottom: normal $P_N$, tangential $P_T$ and normal-tangential $P_N - P_T$, drawn together with $P_N$ and $P_T$. The normal components have a maximum and a minimum while the tangential components have two minima, and the normal-tangential components present two maxima at the interfaces which account for the twice surface tension of the fluid.

## 7. Concluding remarks

The SD phenomenon is of much help in preparing equilibrated liquid–vapour systems with two planar interphases. The fact that the thermodynamic data obtained from this procedure agree with data calculated by other

methods is a strong argument to support the idea of the samples achieving true equilibrium. Specially when confronted with the GEMCS data, since this MC method, in its development requires that the chemical potentials are equal in both phases, even though they do not explicitly appear as variables in the simulation.

The SD phenomenon is of much help in preparing equilibrated liquid–vapour systems with two planar interphases, with a total density near the critical density of the system. Trokhymchuk and Alejandre [18] reported the pressure profiles for the LJ fluid with several cut off distances of the potential, calculated with Monte Carlo and molecular dynamics methods, establishing the unequivocal condition of mechanical equilibrium of the system. It rested to show that the same thing happened to the temperature and chemical potential profiles, to establish the full thermal and chemical equilibrium conditions. This is the main aim of this work. The fact that the thermodynamic data obtained from this procedure agree with data calculated by other methods is a strong argument to support the idea of the samples achieving true equilibrium. It is also a very easy procedure to obtain a planar interphase in a very short time, spinodal decomposition is a picosecond phenomena. An alternative method to prepare a slab of liquid is to initiate the simulation with a normal cubic box at a liquid density until it reaches equilibrium. The cubic box is then stretched taking care that the global density is near the critical density of the fluid. The simulation is allowed to achieve an equilibrium state for the liquid–vapour interface. This procedure takes longer and is more difficult to automate. 'Yet it is necessary to set up and simulate with considerable expense adjoining bulk phases which in some sense do not contribute to the properties of interest. This inefficiency seems to be unavoidable' [16]. For some people this is not enough. A more stringent test of linear temperature, pressure and chemical potential profiles is in order. This test is achieved in this communication, where it is shown that the calculated profiles for two different attractive potential give equivalent linear results, within the statistical noise of the temperature, pressure and chemical potential profiles. Temperature, pressure and chemical potential profiles, for both LJ and SW fluids are quite horizontal, even though the former (LJ) looks noisier because the density intervals used to calculate them were half the size as those used in the SW case. Longer runs were performed to calculate the pressure profile for the LJ system (10 times as long) to make sure that the noise in the figures was just that. Curves black, green and blue in Figure 2 support this point. Longer runs were done only for temperature and pressure only, not for chemical potential which is more costly. Fluctuations in pressure and chemical potential are similar, so conclusions for the pressure profile in terms of statistical errors can be applied to the chemical potential as well.

Longer runs were performed to analyse the pressure for the SW fluid. The maximum and minimum present in this system prevail for this longer runs in contrast to the LJ system where those features disappear as noise once the run is long enough (see Figure 2). Assuming that the features in the SW system pressure are real, even though small, some questions arise. Is the discontinuous nature of the SW potential against the continuous character of the LJ makes the difference? Is the definition of the normal component of the pressure tensor applicable to the interphase or an alternative definition for this region is needed? Is the Clausius' virial theorem applicable across the interphase? More research is needed to answer these questions, that we plan to perform in the near future.

## Acknowledgments

Thanks also to the Super Computer Center of UAM-Iztapalapa for a generous allotment of computing time.

## Disclosure statement

No potential conflict of interest was reported by the authors.

## Funding

Thanks to Conacyt for the grant of Frontiers of Science No. 2015-02-1450 entitled 'Programmable Matter', SEP-CONACYT-178963, RTMCB-2017 and for the scholarship support of A.B.G.

## References

[1] J.P. Hansen and L. Verlet, Phys. Rev. **184** (1), 151–161 (1969).
[2] G.A. Chapela, G. Saville and J.S. Rowlinson, Faraday Discuss. **59**, 22 (1975).
[3] G.A. Chapela, G. Saville, S.M. Thompson and J.S. Rowlinson, J. Chem. Soc. Faraday Trans. **73**, 1133 (1977).
[4] G.A. Chapela, S.E. Martínez-Casas and C. Varea, J. Chem. Phys. **86** (10), 5683–5688 (1987).
[5] M. Rao and D. Levesque, J. Chem. Phys. **65** (8), 3233–3236 (1976).
[6] M. Rao and B.J. Berne, Mol. Phys. **37** (2), 455–461 (1979).
[7] D.J. Adams, Mol. Phys. **37** (1), 211–221 (1979).
[8] J.J. Nicolas, K.E. Gubbins, W.B. Strett and D.J. Tildeley, Mol. Phys. **37** (5), 1429–1454 (1979).
[9] A.Z. Panagiatopoulos, Mol. Phys. **61** (4), 813–826 (1987).
[10] A. Lofti, J. Vrabec and J. Fischer, Mol. Simul. **5**, 233 (1990).
[11] B. Widom, J. Chem. Phys. **39** (11), 2808–2812 (1963).
[12] N.B. Wilding and A.D. Bruce, J. Phys.: Condens. Matter **4** (12), 3087–3108 (1992).
[13] D. Kofke, J. Chem. Phys. **98** (5), 4149–4162 (1993).
[14] G.J. Gloor, G. Jackson, F.J. Blas and E. de Miguel, J. Chem. Phys. **123** (13), 134703 (2005).
[15] A. Ghoufi, P. Malfreyt and D.J. Tildesley, Chem. Soc. Rev. **45** (5), 1387–1409 (2016).

[16] L. Vega, E. de Miguel, L.F. Rull, G. Jackson and I.A. McLure, J. Chem. Phys. **96** (3), 2296–2305 (1992).
[17] A.L. Benavides, J. Alejandre and F. del Río, Mol. Phys. **74** (2), 321–331 (1991).
[18] A. Trokhymchuk and J. Alejandre, J. Chem. Phys. **111** (18), 8510–8523 (1999).
[19] A.R. Imre, G. Mayer, G. Házi, R. Rozas and T. Kraska, J. Chem. Phys. **128** (11), 114708 (2008).
[20] J.K. Singh, D.A. Kofke and J.R. Errington, J. Chem. Phys. **119** (6), 3405–3412 (2003).
[21] L. Verlet, Phys. Rev. **159** (1), 98–103 (1967).
[22] B.J. Alder and T.E. Wainwright, J. Chem. Phys. **31** (2), 459–466 (1959).
[23] D.C. Rapaport, *The Art of Molecular Dynamics Simulation*, 2nd ed., Chap. 14 (Cambridge University Press, New York, NY, 2004).
[24] G.A. Chapela, S.E. Martínez-Casas and J. Alejandre, Mol. Phys. **53** (1), 139–159 (1984).
[25] L.G. MacDowell, V.K. Shen and J.R. Errington, J. Chem. Phys. **125** (3), 034705 (2006).
[26] L.G. Binder, J. Chem. Phys. **125**, 034705 (2010).
[27] F.F. Abraham, D.E. Schreiber and J.A. Barker, J. Chem. Phys. **62** (5), 158 (1975).
[28] J.G. Kirkwood and F.P. Buff, J. Chem. Phys. **17** (3), 338–343 (1949).
[29] F.P. Buff, J. Chem. Phys. **23** (3), 419–427 (1955).
[30] S. Ono and S. Kondo, in *Handbook of Physics*, edited by S. Fltigge (Springer, Berlin, 1960), Vol. 10.
[31] J.P.R. B. Walton, D.J. Tildesley and J.S. Rowlinson, Mol. Phys. **48** (6), 1357–1368 (1983).
[32] G.A. Chapela and J. Alejandre, J. Chem. Phys. **132** (10), 104704 (2010).